

# Flows Driven by a Combination of Source/Sink

## Part 2: Interior Creeping Flows

T. B. A. El Bashir

Department of Mathematics and Statistics  
Sultan Qaboos University, P.O. Box 36  
Al-Khod 123, Sultanate of Oman  
elbashir@squ.edu.om

### Abstract

In this paper, two-dimensional creeping flows generated by source and sink inside a circular cylinder are studied in the presence of different boundary conditions. For simplicity, line source and sink are assumed to be parallel to the cylinder axis, all axes in the same plane. The interior boundary value problem associated with these flows is solved in terms of a stream function. Analytical solutions for the flow field are obtained by straight forward application of the Fourier method. These solutions are used to plot streamline topologies of these flows and the flow patterns are sketched for a number of special cases where the boundary conditions is varying from no slip to perfect slip boundary conditions. Eddies of various sizes and shapes appear as the parameter is varied. Some interesting flow patterns are observed in the parameter space which may have applications in vortex mixing flows.

**Mathematics Subject Classification:** 76D07, 76D99

## 1 Introduction

The first part (El-Bashir 2009 ref[4]; herein referred to as part 1) is investigates flows outside a cylinder for various combinations (strengths and locations) of source and sink. The study of creeping flows is a widely investigated subject due to its relevance to stirring and mixing fluids applications. An insight into various mechanisms and flow topologies of such flows with respect to available free parameters can be beneficial to improving the performance of various systems involving such flows. To gain such insight, it is usually desirable to design models that retain the basic flow feature of the complex problem, yet simple enough to be analyzed accurately using a combination of analysis and numerics. The most common model used to demonstrate stirring process in

the two-dimensional creeping flows generated by source/sink inside a circular cylinder. In these models, a line source and sink, which may be regarded as a mixer or a stirrer, has been used as a model. Incidentally, this flow is topologically equivalent to the flow between two eccentric circular cylinders with inner or both cylinders rotating which models flow in a journal bearing (see [2] for a comprehensive analysis).

In this paper, we include varying boundary conditions to study interior creeping flows induced by source and sink of the type that can be used to model various physical effects. These boundary conditions are more general and allow choices of boundary conditions ranging from no-slip to perfect-slip. There are many situations where such boundary conditions could be more appropriate. For example, if the boundary were coated with polymer. In the presence of such boundary conditions in the interior of a circular cylinder, we derive exact representation of solutions induced by source and sink. Using Fortran, we have explored various flow features of these flows which are discussed later in this paper.

The varying boundary conditions consider here provide the possibilities of a richer and interesting variety of flow patterns as shown in this paper. Some of these interior flows with no-slip boundary condition have been considered by other investigators (see [7] and [5]). The work of [7] and [5] have shown the existence of attached eddies in some cases. The flow patterns possible in these studies are limited by the fact that the fluid does not slip at the surface.

The paper presents a collection of formulae, derived here for the first time, and streamline topologies for various positions of source and sink driven two-dimensional creeping flows inside a circular cylinder which include the effect of slip boundary conditions.

The paper is organized as follows. In section 2, the basic equations are given and using the Stokes stream function the problem is reformulated. The boundary conditions are then derived in terms of stream function and a brief discussion on the no-slip constraints is provided. In section 3, the general solution is derived by the use of Fourier expansion method. The solutions to various singularity driven flow problems are presented in section 4 and 5. The basic singularities considered here include single and double stokeslets. The effect of no-slip on the flow fields is discussed in each case. The flow description is illustrated in different situations through streamline plots. The concluding remarks of the present analysis are presented in section 6.

## 2 Mathematical preliminaries

For two-dimensional creeping flow the (non-dimensional) governing equation and boundary conditions are broved from part 1 [4] as

$$\nabla^4 \psi = 0, \quad (1)$$

Subject to the boundary conditions

- (i). Normal velocity is zero on the boundary i.e.,  $q_r = 0$  on  $r = a$ .
- (ii). Tangential velocity is proportional to the tangential stress at the surface of the cylinder i.e.,  $q_\theta = \frac{\lambda}{\mu} T_{r\theta}$ , where

$$T_{r\theta} = \mu \left[ \frac{1}{r} \frac{\partial q_r}{\partial \theta} + r \frac{\partial}{\partial r} \left( \frac{q_\theta}{r} \right) \right], \quad (2)$$

Is the tangential stress and  $\lambda \geq 0$  is the slip coefficient. In terms of stream function, these conditions become

$$\psi = 0 \quad \text{and} \quad \frac{\partial \psi}{\partial r} = \lambda r \frac{\partial}{\partial r} \left( \frac{1}{r} \frac{\partial \psi}{\partial r} \right), \quad \text{on } r = a. \quad (3)$$

In the present paper, we investigate the flows induced by a combination of line source and sink inside a circular cylinder.

### 3 Method of solution

There are classical and numerical methods to solve (1) subject to the boundary conditions (3). The most suitable and commonly used technique is the Fourier expansion method. In this method, the given flow is expanded in a Fourier series with known Fourier coefficients. Then, the unknown coefficients of the perturbed flow (also written in a Fourier series) are computed with the aid of the boundary conditions. The other methods applicable to the present problem include the image method ([3], [1]) and the boundary integral equation method [6]. We adopt the Fourier representation technique for our problem and make an attempt to sum the resulting series solution. To this end, we write the given flow field in the absence of the cylinder as

$$\psi_0 = G(r) + \sum_{n=1}^{\infty} \left[ \frac{\alpha_n}{r^n} + \frac{\beta_n}{r^{n-2}} \right] f_n(\theta). \quad (4)$$

Here,  $f_n(\theta) = a_n \cos n\theta + b_n \sin n\theta$ , and  $\alpha_n, \beta_n, a_n, b_n$  are known constants. The function  $G(r)$  is a known function of  $r$  alone associated with the given flow. The Fourier representation of the complete solution in the interior domain can be taken as

$$\psi = \psi_0 + A_0 + B_0 r^2 + \sum_{n=1}^{\infty} [A_n r^n + B_n r^{n+2}] f_n(\theta). \quad (5)$$

The constants  $A_0$  and  $B_0$  satisfying the boundary conditions will be found later. The unknown Fourier coefficients  $A_n$  and  $B_n$  for  $n \geq 1$  may be calculated separately by applying the boundary condition. These coefficient are given by

$$a^n A_n = \frac{(n+1)(1-\lambda_1)\alpha_n/a^n + (n\beta_n/a^{n-2})(1-2\lambda_1)}{n\lambda_1 - 1 + \lambda_1}. \quad (6)$$

$$a^{n+1} B_n = -\frac{(n-1)(1-\lambda_1)\beta_n/a^{n-1} + (n\alpha_n/a^{n+1})}{n\lambda_1 - 1 + \lambda_1}. \quad (7)$$

where  $\lambda_1 = 2\lambda/(1+2\lambda)$ ,  $0 \leq \lambda_1 \leq 1$ . The corresponding coefficients for a rigid cylinder with no-slip and perfect-slip boundary conditions may be obtained from (6) and (7) by setting  $\lambda_1 = 0$  and  $\lambda_1 \rightarrow 1$  respectively

## 4 Source and sink

We now employ the solution scheme derived in the previous section (equations (4)-(7)) to source and sink in the presence of a cylinder. We show that the Fourier series solution can be summed to yield closed form expressions for the stream function.

The stream function of the flow induced by a sink of strength  $\Gamma_1$  located at  $r = c$ ,  $\theta = 0$  is given by

$$\psi_0 = \Gamma_1 \tan^{-1} \left( \frac{r \sin \theta}{c - r \cos \theta} \right). \quad (8)$$

For  $r > c$ , above expression may be expanded in the form

$$\psi_0 = \Gamma_1 \sum_{n=1}^{\infty} \frac{c^n}{nr^n} \sin(n\theta). \quad (9)$$

From (4) and ((7), we obtain

$$G(r) = 0, \quad \alpha_n = \frac{\Gamma_1 C^n}{n}, \beta_n = 0 \quad \text{for all } n \geq 1. \quad (10)$$

Since  $G(r) = 0$ , the coefficients  $A_0$  and  $B_0$  vanish in the present case. The coefficients  $A_n$  and  $B_n$  for a source flow after the introduction of a cylinder are

$$A_n = -\frac{1}{n\lambda_1 - 1 + \lambda_1} \left[ (n+1)(1-\lambda_1) \frac{\alpha_n}{a^{2n}} \right], \quad (11)$$

$$B_n = \frac{1}{n\lambda_1 - 1 + \lambda_1} \left[ \frac{n\alpha_n}{a^{2n+2}} \right]. \quad (12)$$

The stream functions for the source and the sink are shown in details in the proceeding subsection.

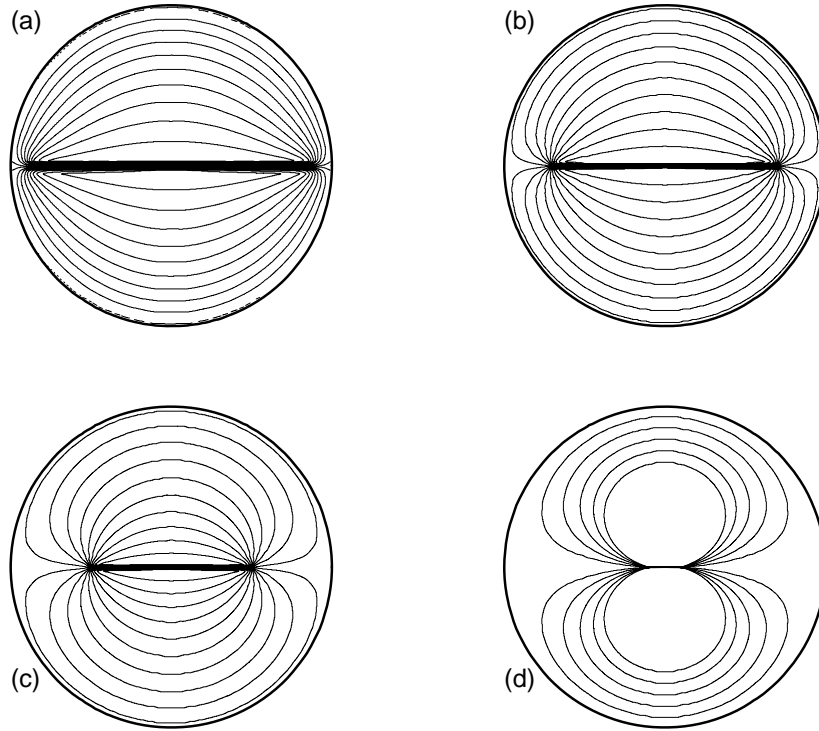


Figure 1: Flow generated by a source and sink ( $\lambda_1 = 0$ ,  $\Gamma_1 = -\Gamma_2 = 1$ ) for different positions (a)  $c = \hat{c} = 0.9$  (b)  $c = \hat{c} = 0.7$  (c)  $c = \hat{c} = 0.5$  (d)  $c = \hat{c} = 0.1$ .

#### 4.1 no-slip boundary condition

By setting  $\lambda_1 = 0$ , Fourier series solution with the constants given in (11) and (12) may be summed to yield the following closed form expression:

$$\psi = \Gamma_1 \left[ \tan^{-1} \left( \frac{r \sin \theta}{c - r \cos \theta} \right) - \tan^{-1} \left( \frac{\sin \theta}{rc - \cos \theta} \right) \right]. \quad (13)$$

By using standard techniques for source of strength  $\Gamma_2$  at  $r = \hat{c}$  and  $\theta = \pi$  we get

$$\psi = \Gamma_2 \left[ \tan^{-1} \left( \frac{r \sin \theta}{\hat{c} + r \cos \theta} \right) - \tan^{-1} \left( \frac{\sin \theta}{r\hat{c} + \cos \theta} \right) \right]. \quad (14)$$

The no-slip boundary conditions does not change the flow qualitatively as shown in some representative plots in figure 1. The flow in all cases consists of two eddies separated by a dividing streamline ( $\psi = 0$ ) whose end points are

resting on the wall of the cylinder. The shape of the eddies, depend on the source and the sink locations. Figure 1 above shows streamline patterns for the case of equidistant ( $c = \hat{c}$ ) for several choices of  $c$ . For  $c=0.9$  near the wall a symmetric pair of eddies appear as shown in figure 1(a). Initially the large eddy extends up to the wall and start shrinking while moving inward towards the center. Some of this scenario is shown in figure 1(a)-(d).

## 4.2 general boundary condition

For general  $0 < \lambda_1 < 1$ , Fourier series solution with the constants given in (11) and (12) may be summed by standard techniques, to get

$$\psi = \Gamma_1 \left[ \tan^{-1} \left( \frac{r \sin \theta}{c - r \cos \theta} \right) - \tan^{-1} \left( \frac{\sin \theta}{rc - \cos \theta} \right) - \frac{(r^2 - 1)I_{si}}{c\lambda_1} \right]. \quad (15)$$

where

$$I_{si} = \frac{r^{\frac{(1-\lambda_1)}{\lambda_1}}}{\lambda_1} \int_0^r \frac{\sin \theta \rho^{\frac{(\lambda_1-1)}{\lambda_1}}}{\rho^2 - 2c\rho \cos \theta + c^2} d\rho$$

and similarly for source at  $r = \hat{c}$  and  $\theta = \pi$

$$\psi = \Gamma_2 \left[ \tan^{-1} \left( \frac{r \sin \theta}{\hat{c} + r \cos \theta} \right) - \tan^{-1} \left( \frac{\sin \theta}{r\hat{c} + \cos \theta} \right) - \frac{(r^2 - 1)I_{so}}{\hat{c}\lambda_1} \right]. \quad (16)$$

where

$$I_{so} = \frac{r^{\frac{(1-\lambda_1)}{\lambda_1}}}{\lambda_1} \int_0^r \frac{\sin \theta \rho^{\frac{(\lambda_1-1)}{\lambda_1}}}{\rho^2 + 2\hat{c}\rho \cos \theta + \hat{c}^2} d\rho$$

Figures 2(a)-(d) show flow patterns for an increasing sequence of  $\lambda_1$  when a source and a sink are located at distances  $x = 0.5$  and  $x = -0.75$ , respectively. First, a symmetric pair of secondary eddies appears with their centers almost aligned on the  $y$ -axis. This is shown in Figure 2 (a) for  $\lambda_1=0.4$ . With increasing values of  $\lambda_1$ , these eddies tilt to the right and start moving towards the line joining the source and the center of the cylinder. Figure 2 (b) shows this for a typical value of  $\lambda_1=0.45$ . A small flow region near the line joining the sink and the center of the cylinder ensues where the fluid seems to flow from the center to the sink. Rest of the flow seems to contain a recirculating zone surrounded by fluid flowing from the source to the center. With further increases in the value of  $\lambda_1$ , the flow region between the center and the sink grows in size where as the rest of the flow region shrinks in size as seen in figure 2 (c) for  $\lambda_1=0.55$ .

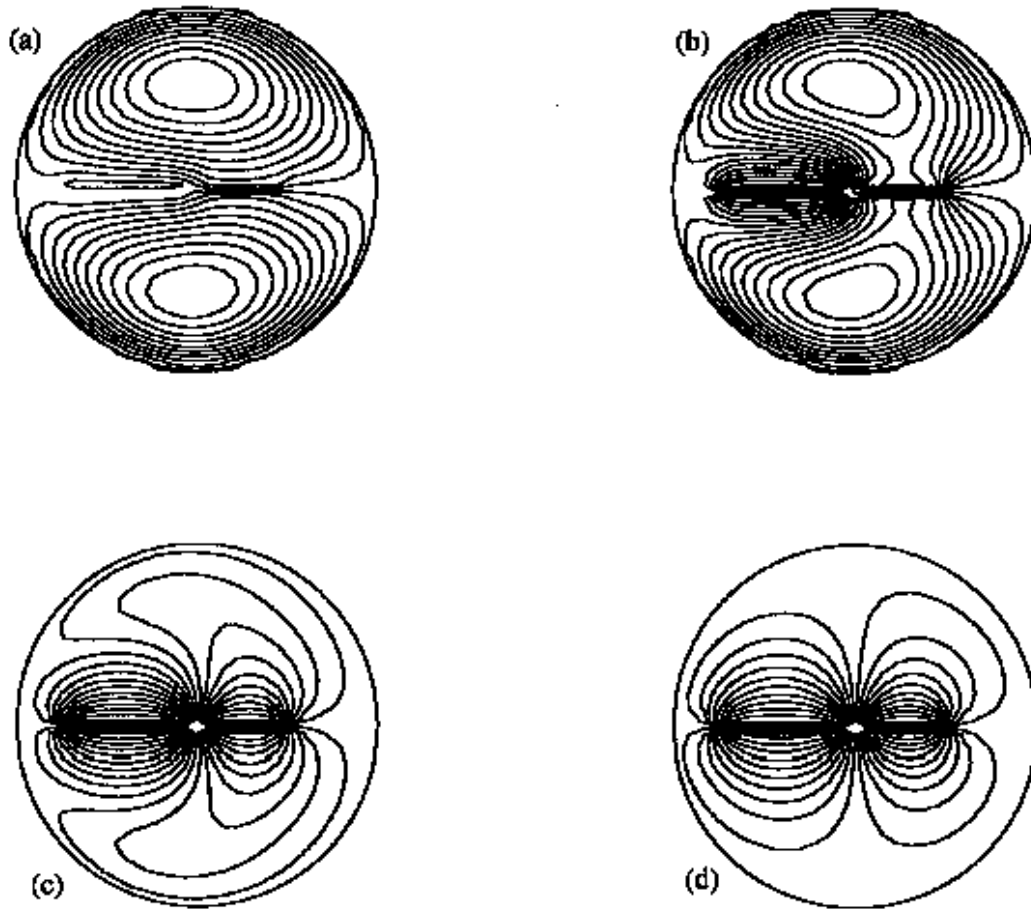


Figure 2: Flow generated by a source and sink at ( $c = 0.5$ ,  $\hat{c} = 0.75$ ) for various values of  $\lambda_1$ . Here  $\Gamma_1 = -\Gamma_2 = 1$  (a)  $\lambda_1 = 0.4$  (b)  $\lambda_1 = 0.45$  (c)  $\lambda_1 = 0.55$  (d)  $\lambda_1 = 0.9$ .

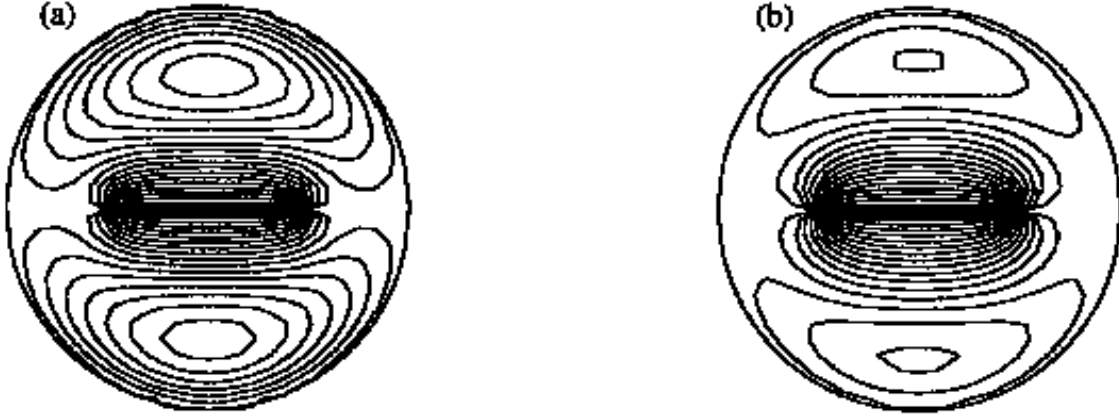


Figure 3: Flow generated by a source and sink at  $(c = 0.5, \hat{c} = 0.5)$  for various values of  $\lambda_1$ . Here  $\Gamma_1 = -\Gamma_2 = 1$  (a)  $\lambda_1 = 0.2$  (b)  $\lambda_1 = 0.4$ .

Eventually, at  $\lambda_1=0.9$ , a dipole-type flow ensues at the origin.

If a source and a sink are located equidistant ( $c = \hat{c} = 0.5$ ) from the center along a diagonal, then the flow structure (See figures 3(a)-(b)) changes little. An increase in the value of  $\lambda_1$  in this case pushes the eddies towards the wall.

### 4.3 perfect-slip boundary condition

By taking the limit  $\lambda_1 \rightarrow 1$ , in (15) the solution may be reduces to

$$\psi = \Gamma_1 \left[ \tan^{-1} \left( \frac{r \sin \theta}{c - r \cos \theta} \right) - r^2 \tan^{-1} \left( \frac{\sin \theta}{rc - \cos \theta} \right) \right]. \quad (17)$$

and similarly for source equation (16)

$$\psi = \Gamma_2 \left[ \tan^{-1} \left( \frac{r \sin \theta}{\hat{c} + r \cos \theta} \right) - r^2 \tan^{-1} \left( \frac{\sin \theta}{r\hat{c} + \cos \theta} \right) \right]. \quad (18)$$

Figures 4 (a)-(c) show flow patterns for a decreasing sequence of values of equidistant  $c = \hat{c}$  when a source strength  $\Gamma_1$  is double a sink strength  $\Gamma_2$ . First, a symmetric pair of eddies appears with their centers almost aligned on the  $y$ -axis. this is shown in Figure 4(a) for  $c = \hat{c} = 0.5$ . With decreasing values of  $c = \hat{c}$  these eddies tilt to the right and start moving towards the line joining



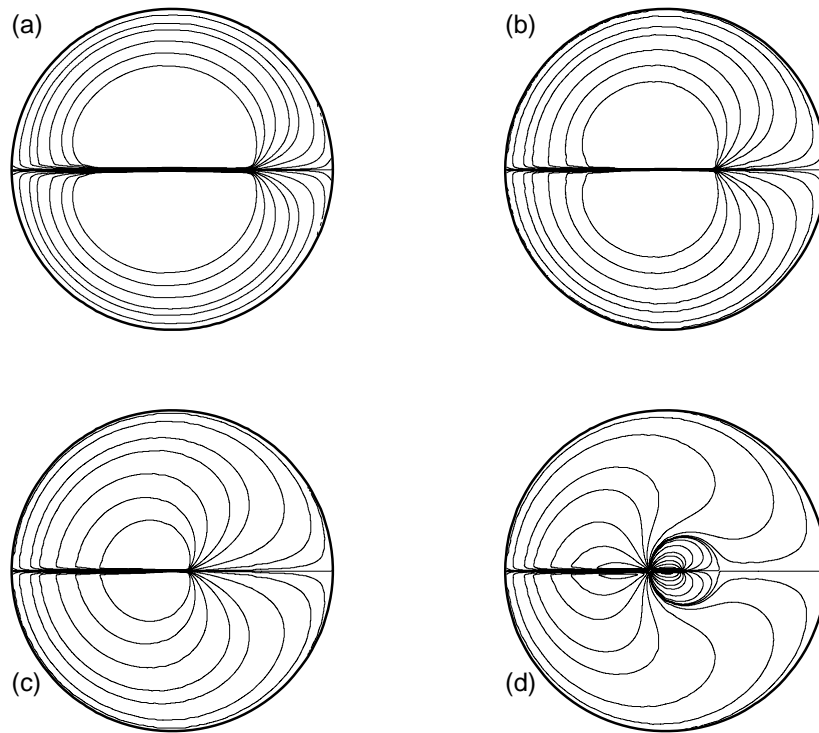


Figure 4: Flow generated by a source and sink ( $\lambda_1 = 1$ ) for different strength and same streamlines  $\psi = -2.5, -2, -1.5, -1, -0.7, -0.3, -0.09, -0.02, 0, 0.02, 0.09, 0.3, 0.7, 1, 1.5, 2, 2.5$  (a)  $\Gamma_1 = 2, \Gamma_2 = -1, c = \hat{c} = 0.5$  (b)  $\Gamma_1 = 2, \Gamma_2 = -1, c = \hat{c} = 0.3$  (c)  $\Gamma_1 = 2, \Gamma_2 = -1, c = \hat{c} = 0.1$  (d)  $\Gamma_1 = 1, \Gamma_2 = -2, c = \hat{c} = 0.1$

the source and the center of the cylinder. Figures 4(b) and 4(c) shows this for a typical values of  $c = \hat{c} = 0.3$  and  $c = \hat{c} = 0.1$ , respectively. For fixed  $c = \hat{c}$ , we can compare 4(c) and 4(d). In 4(d) the sink strength  $\Gamma_2$  is double a source strength  $\Gamma_1$ , the flow seems to contain a recirculating zone surrounded by fluid flowing from the source to the center.

## 5 CONCLUSION

We have demonstrated here the effect of slip on steady flows inside an infinitely long cylinder induced by source and sink, using three types of boundary conditions. In each of these cases, an exact solution for the stream function has been derived in closed form which have been subsequently used to plot streamline topologies for these flows. These shed light on the qualitative features of the flows such as eddies. In all cases, eddies of different sizes and shapes are found to occur. The streamline plots illustrate the existence of interior saddle points (hyperbolic points) in these flows. The hyperbolic points depend on both slip as well as the location of the source and the sink.

In the case of equal strength ( $\Gamma_1 = -\Gamma_2$ ), both the slip parameter and the locations have significant effects on the flow patterns. The cores of the eddies in these flows move closer to the source or the cylinder wall depending on whether the primary source and sink are located at equidistance from the origin or otherwise. This flow model might be used in certain processes involving simultaneous suction and injection of a fluid. Finally, analytical results and the streamline topologies presented here may inspire one to design new experiments on mixing or chaos, and also to use these for validating numerical simulations on such flows in bounded domains.

## 6 ACKNOWLEDGMENT

This research has been supported by Sultan Qaboos University.

## References

- [1] A. Avudainayagam and B. Jothiram, "No-slip images of certain line singularities in a circular cylinder," *Int. J. Eng. Sci.* 25, 1193 (1987).
- [2] B. Y. Ballal and R. S. Rivlin, "Flow of a Newtonian fluid between eccentric rotating cylinders: Inertial effects," *Arch. Ration. Mech. Anal.* 62, 237

(1976).

- [3] J. M. Dorrepaal, M. E. O'Neill, and K. B. Ranger, "Two-dimensional Stokes flows with cylinders and line singularities," *Mathematika* 31, 65 (1984).
- [4] T.B.A. El Bashir, "Flows driven by a combination of Source/Sink: Part 1. exterior creeping flows," *APPLIED MATHEMATICAL SCIENCES*, submitted.
- [5] V. V. Meleshko and H. Aref, "A blinking vortex model for chaotic advection," *Phys. Fluids A* 8, 3215 (1996).
- [6] H. Power, "The completed double layer boundary integral equation method for two-dimensional Stokes flow," *IMA J. Appl. Math.* 51, 123 (1993).
- [7] K. B. Ranger, "Eddies in two-dimensional Stokes flow," *Int. J. Eng. Sci.* 18, 181 (1980).

**Received: January, 2009**